Surface modification of Ti45Nb alloy by immobilization of RGD peptide via self assembled monolayer

G. Zorn · I. Gotman · E. Y. Gutmanas ·
R. Adadi · C. N. Sukenik

Abstract A new low modulus β Ti-Nb alloy with low elastic modulus and excellent corrosion resistance is currently under consideration as a surgical implant material. The usefulness of such materials can be dramatically enhanced if their surface structure and surface chemistry can be controlled. This control is achieved by attaching a self assembled monolayer (SAM) based on 11-chloroacetyl-1-undecylphosphonic acid, CAUDPA, to the surface and immobilization of a peptide to the monolayer. The SAM is characterized by Fourier Transform Infrared Spectroscopy (FTIR) and X-ray Photoelectron Spectroscopy (XPS) at two different takeoff angles. The CAUDPA molecules were covalently bonded on the substrate in a configuration in which the phosphonic group turns toward the Ti45Nb while the acetyl chloride end group tail turns to the topmost surface. In such configuration sequential in situ reaction is possible by exchange between the chloride and a biological molecule. Such biological molecule is the arginine-glycine-aspartic acid-cysteine, RGDC, small amino acid sequence present in many molecules of the extracellular matrix. Preliminary cell culture in-vitro result shows an improvement of the response of osteoblast cells to Ti45Nb after the peptide immobilization.

G. Zorn · I. Gotman (✉) · E. Y. Gutmanas
Faculty of Materials Engineering, Technion, Haifa, Israel
e-mail: gotman@tx.technion.ac.il

R. Adadi · C. N. Sukenik
Department of Chemistry, Bar-Ilan University, Ramat-Gan, Israel

Introduction

The use of titanium and its alloys as biomaterials is constantly increasing due to their relatively low modulus and good corrosion resistance. Also, titanium is remarkably compatible with human tissue as compared to other metals. These properties were the driving force for the introduction of commercially pure (cp) Ti and two-phase $\alpha+\beta$ (Ti-6Al-4 V) alloys into orthopedic surgery, as well as for the more recent development of high-strength low-stiffness single-phase β-Ti alloys. Of this last group, β-(Ti-Nb) alloys are especially noteworthy due to their excellent corrosion resistance and remarkably low elastic modulus that reduces stress shielding [1–3]. Successful integration of Ti-Nb (as well as other Ti alloy) implants in bone relies on their bone-regenerating capability. In this respect, Ti alloys are inferior to bioactive materials such as bioglasses and calcium-phosphate ceramics (e.g. hydroxyapatite, β-tricalcium phosphate). It has been suggested, however, that since the biological response to an implanted biomaterial is influenced by the material's surface properties [4, 5], the integration of Ti alloy implants in the surrounding bone tissue can be improved by modifying the alloy surface. One approach is the immobilization of biological molecules (growth factors, adhesive proteins) onto the implant surface in order to induce a specific cellular response and promote osteo-integration. The application of large extracellular matrix proteins, however, can be unpractical due to their low chemical stability, solubility in biological fluids and high cost. In addition, entire ECM molecules are usually of allogeneic or xenogeneic origin and thus associated with the risk of immune reaction and pathogen transfer. An alternative approach, therefore,

is the application of short amino acid sequences—peptides—that can mimic the cell attachment activity of the entire protein. One such sequence that has been identified as the mediator of cell recognition and attachment is an RGD (Arg-Gly-Asp) domain [6, 7]. Small RGD-containing peptides are relatively stable and can be synthesized with high levels of purity and controlled chemical composition.

The attachment of biomolecules to metallic surface can be achieved using self-assembled monolayers (SAMs) as cross-linkers. SAMs provide chemically and structurally well-defined surfaces that can often be manipulated using standard synthetic methodologies [8]. Thiol on gold SAMs [9, 10] and siloxane-anchored SAMs [11] have been particularly well-studied. A problem related to the application of immobilized biomolecules via silanization techniques is the hydrolysis of the siloxane films when exposed to aqueous (physiological) conditions [12]. More recently, alkyl phosphate films that remain robust under physiological conditions [13] have been used to provide an ordered monolayer on tantalum oxide surfaces [14, 15], and alkylphosphonic acids have been used to coat the native oxide surfaces of metals (and their alloys) including iron [16], steel [17] and titanium [18].

In the present paper, a procedure for RGD-containing peptide attachment to the surface of a low modulus Ti-Nb alloy using an alkylphosphonic acid monolayer as a cross linker is reported, and the effect of the RGD coat on osteoblast attachment is evaluated.

Materials and methods

Surface preparation and peptide grafting

Ti-45 wt.% Nb alloy was purchased from Performance Alloys and Materials, Ltd. (New Jersey, U.S.A). 11-chloroacetyl-1-undecylphosphonic acid (CAUDPA) was synthesized at Department of Chemistry, Bar-Ilan University. RGDC (Arg-Gly-Asp-Cys) peptide was purchased from Biotest Ltd, Kfar Saba, Israel. 3 mm thick 10×10 mm^2 and 10×25 mm^2 plates were cut from Ti45Nb sheet and ground finishing with 1,200 grit silicon carbide paper. This was followed by electro-polishing and anodic oxidation in 1M H_2SO_4 at room temperature [19, 20]. The current density was kept at 60 mA/cm^2 while the potential was allowed to increase from 5 V to a preset value of 100 V. Anodized specimens were sonicated with CH_2Cl_2, acetone, ethanol, and DI water for 15 min each, and then dried in a stream of dry air.

Peptide grafting onto the Ti alloy surface involved two stages (Fig. 1): (i) attachment and self-assembly of CAUDPA on the metallic surface; (ii) reaction of the CAUDPA chloroacetyl functionality with the thiol group present in the terminal cystein of the RGDC peptide. Experimental procedure for Ti45Nb bio-functionalization was as follows:

CAUDPA SAM (Self-Assembled Monolayer) deposition

17 mg CAUDPA were dissolved in 40 mL of tetrahydrofuran (THF) and heated (with stirring) to 70°C under nitrogen [21]. Into this solution, anodized Ti45Nb coupons were immersed for 2 h after which the temperature was raised to 120°C causing THF to boil out after ~2 h. The specimens were left in open air at 120°C for additional 16 h, rinsed in fresh dry THF and then dried in filtered N_2. The above procedure was previously shown to produce robust SAMs of hexadecylphosphonic acid (HDPA) covalently attached to the surface of Ti45Nb alloy via their phosphonate functionality [22].

Peptide immobilization

A solution of RGDC (2 mM) was prepared in 10 mL of double distilled water. CAUDPA SAM-coated

Fig. 1 Schematic of RGDC peptide grafting on Ti45Nb surface: (a) attachment and self-assembly of CAUDPA on the metallic surface; (b) reaction of the CAUDPA chloroacetyl functionality with the thiol group of the terminal cystein in RGDC
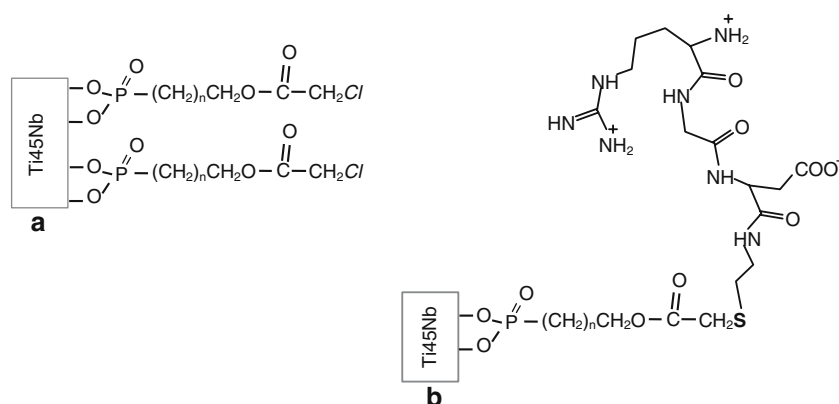
specimens were immersed into the stirred peptide solution at room temperature for 24 h, then sonicated with water, dried in filtered nitrogen and sterilized in 70% ethanol for 30 min.

Surface characterization

X-ray Photoelectron Spectroscopy (XPS) analyses were performed on a Sigma probe X-ray photoelectron spectrometer from Thermo V G. Scientific using a monochromatized aluminum anode X-ray source (Al Kα 1486.68 eV). Spectra were taken at two emission angles: $15.5 \pm 7.5°$ (surface sensitive mode) and $59.5 \pm 7.5°$ (bulk mode) takeoff angles with respect to the surface. Samples were analyzed with pass energy of 100.0 eV for survey scans and 20.0 eV for high resolution elemental scans. The energy scale was calibrated by referencing the main hydrocarbon peak which was set at a binding energy of 285.0 eV [23].

Contact angle values (average of at least five measurements taken at different points on the surface) were measured using a Rame-Hart Model 100 Contact Angle Goniometer.

Fourier Transform Infrared Spectroscopy (FTIR) spectra were measured using a Bruker Vector 22 equipped with a Mercury Cadmium Tellurium (MCT) detector. The samples were placed in a Bruker grazing angle accessory. The angle of incidence was 55°. Prior to collection of the spectra, the sample compartment was purged with dried air for 10 min. The spectra (1,000 scans) were then acquired using 4 cm^{-1} resolution and triangular apodization. Each spectrum of CAUDPA SAM-coated samples was obtained by subtracting a background obtained using a clean, bare alloy sample.

Cell culture

Osteoblasts were isolated from calvariae of 1-day-old Sprague-Dawley rats by sequential enzymatic digestion previously described in [24]. Briefly, 40 calvariae were minced and incubated at 37°C for 20 min with gentle shaking in 3 ml of an enzymatic solution containing 0.1% collagenase, 0.05% trypsin, and 4 mM sodium ethylenediaminetetraacetic acid (EDTA) in calcium- and magnesium-free phosphate-buffered saline (PBS). Cells from the first digest were discarded. The procedure was repeated five times, and cells obtained from the last five digests were pooled and cultured in a 25 cm^2 polystyrene cell culture flasks (Corning Inc., Corning, NY, USA) under standard conditions (95% air/5% CO$_2$/37°C) in α-modified minimum essential medium (α-MEM) supplemented with L-glutamine (Biological Industries, Beit Haemek, Israel) containing 10% heat inactivated fetal bovine serum (FBS) and antibiotics (100 mg/mL of penicillin G and 100 IU/mL of strepto-mycin). After reaching confluence, cells were released from the flasks with 0.05% trypsin in EDTA, pooled and suspended in α-MEM medium supplemented with 10% FBS, 5 mmol/L β-glycerophosphate, 50 µg/mL ascorbic acid and antibiotics at a density of 100,000 cells/0.1 ml.

RGDC-coated and uncoated Ti45Nb specimens ($10 \times 10 \times 3$ mm) were sterilized in 70% ethanol for 30 min, air dried in a sterile culture hood and then placed in 24 well tissue culture dishes (Nunc, Roskilde, Denmark). 100,000 cells were seeded on the surface of each specimen and incubated at 37°C for 10 min, after which 2 ml of the enriched α-MEM medium were added. Following gentle shaking, the cells were cultured at 37°C for 7 days. The medium was first changed after 24 h and then every other day. After 7 days culturing the medium was removed and specimens rinsed with PBS. The cells were fixed for 10 min at room temperature in 4% para formaldehyde and stained with 0.1% toluidine blue (Fluka, Buchs, Switzerland). Cell images were taken by optical microscope in reflection mode. Some specimens were coated with a thin gold layer and observed in a scanning electron microscope (SEM).

Results and discussion

Electro-polishing and anodizing of Ti45Nb produced a smooth wavy surface, Fig. 2, with an average roughness (Ra) of 44.7 nm [25]. The anodic oxide thickness was 280 nm [25]. When coated with the chloroacetyl-terminated SAM, the Ti45Nb surface became relatively hydrophobic with contact angles ranging from $66 \pm 3°$(SD) to $52 \pm 4°$ for the advancing and receding angle, respectively. The strong hysteresis suggests a certain degree of disorder of the organic coat (compared, for example, with the well-ordered HDPA SAM on the Ti45Nb surface [22]).
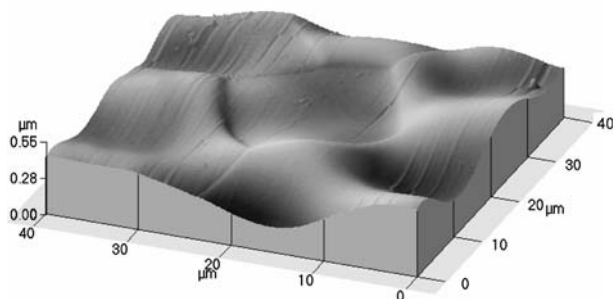

Fig. 2 AFM 3-D image of anodized Ti45Nb
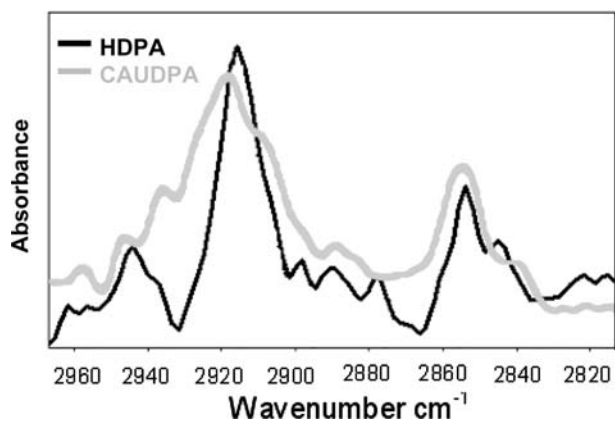
Fig. 3 FTIR spectra of the CAUDPA (gray) and HDPA (black) coated Ti45Nb

In Fig. 3, external reflection FTIR spectrum of CAUDPA SAM-coated Ti45Nb is shown as compared to the previously reported spectrum of Ti45Nb coated by a non-functional HDPA SAM [22]. The position of methylene stretching frequencies is an important diagnostic for the packing of the SAM. Asymmetric C–H stretches of 2917 cm^{-1} or less indicate an ordered, more crystalline film with its methylene groups predominantly in an all-trans conformation [19]. Absorptions at 2922 cm^{-1} or higher reflect a disordered (liquid-like) film. Similarly, lower frequency symmetric C–H stretches (~2850 cm^{-1}) suggest a higher degree of order. The peaks at 2918 cm^{-1} and 2850 cm^{-1} observed in the spectrum of the CAUDPA coated sample suggest a well-organized albeit slightly disordered SAM. It is clear that the HDPA SAM is a better-ordered film. Higher frequencies and broader peaks for the C–H stretches of the CAUDPA monolayer accentuate the difference in the order and packing of the SAMs. The ongoing optimization of the SAM deposition procedure is expected to yield a fully ordered CAUDPA film on Ti45Nb surface.

Figure 4a, b shows XPS spectra of the CAUDPA coated sample collected in the surface sensitive and bulk modes. The peaks are assigned in Table 1. For comparison, XPS spectrum of uncoated (bare) Ti45Nb collected in the bulk mode is given in Fig. 4c. One can see that the peaks of phosphorous and chlorine are only detected in the CAUDPA-coated Ti45Nb and that the Ti2p$_{3/2}$ and Nb3d$_{5/2}$ peaks in this sample are significantly smaller compared to the uncoated one. These observations confirm the presence of a CAUDPA layer on the coated sample surface. Another important observation of the XPS analysis is the reduction of the Cl$_{2p}$ peak area as a function of XPS exposure time, Fig. 5, suggesting that the exposure to
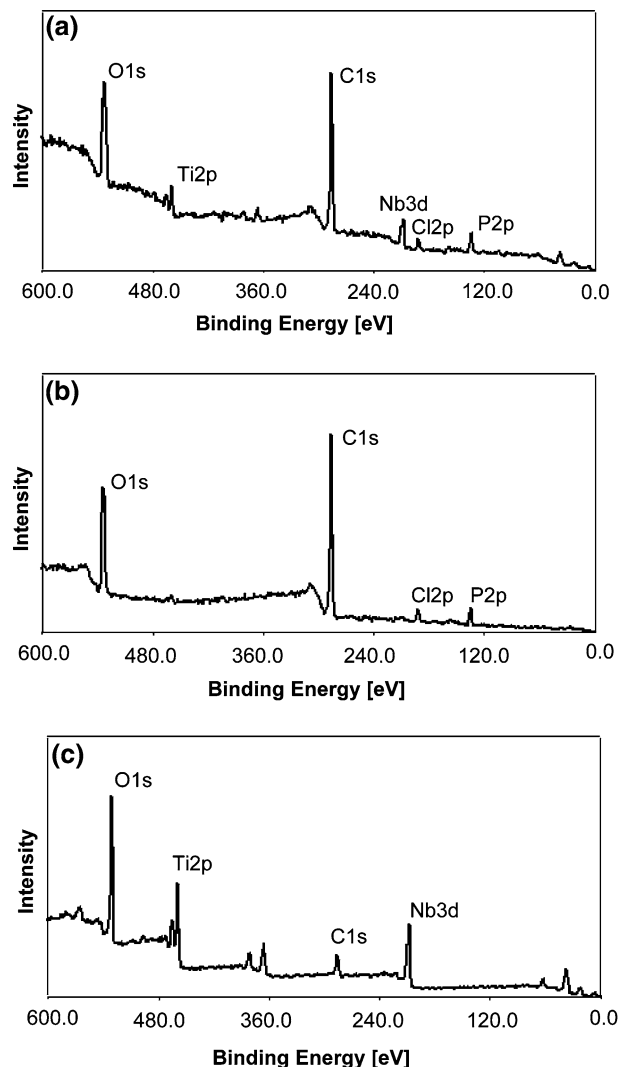
**Fig. 4** XPS spectra of CAUDPA coated Ti45Nb in the bulk (**a**) and surface sensitive (**b**) modes, and of bare anodized Ti45Nb in the bulk mode (**c**)

X-ray irradiation damages the CAUDPA coat. The fact that only chlorine is affected whereas the amounts of carbon, oxygen and phosphorus remain unchanged could be indicative of the "tails-up" SAM configuration with the chloroacetyl functionalities facing the free surface.

When discussing the obtained XPS results one should have in mind that, in addition to the discussed reduction of the chlorine peak, X-ray irradiation can possibly affect the chemical state (binding energies) of the elements thereby limiting our ability to quantitatively analyze the monolayer. The situation is further complicated by the high noise-to-signal ratio caused by the relatively high substrate roughness. Nevertheless, the data are useful for drawing some general conclusions regarding the nature of the organic coat on the
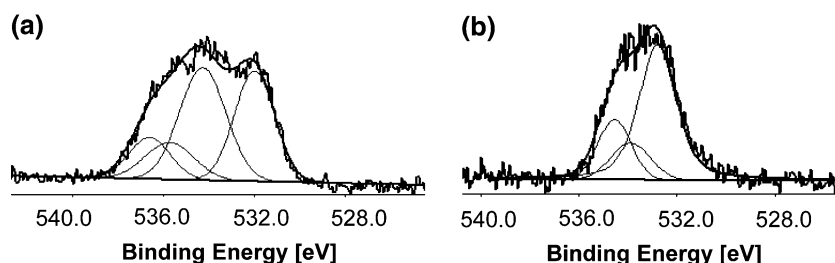
Table 1 Surface elements chemical state and atomic percentage from XPS analysis

Peak	Binding energy [eV]	Assignment	Composition, [at.%]	
			Bulk mode	Surface sensitive mode
C1s	285–289	CH_2; C=O; C–O; C–Cl	63.3	70.9
O1s	530.1	TiO_2; Nb_2O_5	8.3	–
	531.9	P=O; C=O; P–O–Ti; P–O–Nb	9.9	14.4
	533.0	P–O–H	3.5	3.4
	533.65	C–O–C	3.3	4.7
Ti $2p_{3/2}$	458.2	TiO_2	2.3	–
Nb $3d_{5/2}$	208.0	Nb_2O_5	1.7	–
P $2p_{3/2}$	133.2	R–P(O)(OH)$_2$	6.4	5.4
Cl $2p_{3/2}$	200.1	CH_2–Cl	1.3	1.2
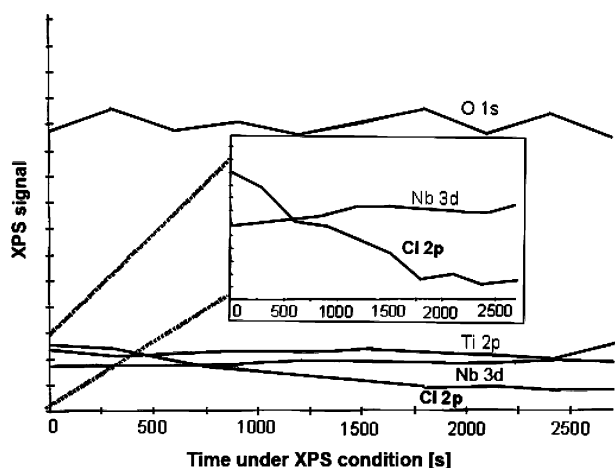
Fig. 5 XPS signals of the surface elements as a function of exposure time to X-ray irradiation

Ti45Nb surface. Thus, the absence of the Ti and Nb peaks in the XPS spectrum collected in the surface sensitive mode (Fig. 4b) suggests that we only see the organic layer at the lower takeoff angle. The C:P ratio of 70.9:5.4 or 13.1 observed in this mode (Table 1) is exactly what is to be expected for a SAM based on CAUDPA.

Figure 6 shows curve-fitted high resolution XPS O1s signals of the CAUDPA-modified sample collected in the surface sensitive and bulk modes. The O1s signal in the bulk mode, Fig. 6a, is quite different from the one detected in the surface sensitive mode, Fig. 6b. The signal collected in the surface sensitive mode can be

nicely fit using only three peaks, while four peaks are needed to fit the bulk mode signal. This fourth peak (530.1 eV) corresponds to the metal oxides (TiO_2 and Nb_2O_5). The absence of this peak in the surface sensitive mode and the fact that we only see the SAM in the surface sensitive mode analysis is consistent with the SAM fully covering the surface. Confirmation that the CAUDPA coating is quite complete is based on the absence of the titanium and niobium peaks at the lower takeoff angle along with the ability to detect them at the higher takeoff angle (Table 1).

The binding energy value of the oxygen O1s at 531.9 eV can be assigned to P=O, C=O, and/or P–O–Ti and P–O–Nb, while the O1s peak at 533.0 eV is assigned to P–O–H. The ratio between the two oxygen peaks (at 531.9 and 533.0 eV) for HDPA SAM on Ti45Nb is 2.8 and 4.3 in the bulk and surface sensitive mode, respectively (Table 1). This ratio speaks to the details of the interaction of the phosphonate with the surface. For an unbound phosphonic group (-P(O)(OH)$_2$), the ratio between P=O and P–OH should be 0.5. Taking into account the contribution of the other double bound oxygen (one C=O per CAUDPA molecule) to the 531.9 peak, the ratio between the two peaks should be 1.0. The much larger proportion of the 531.9 eV peak in the O1s signal from CAUDPA SAM on Ti45Nb is indicative of the strong presence of the P–O–Ti and P–O–Nb bonds. This suggests that CAUDPA molecules have covalently attached to the titanium-niobium oxide surface via transformation of many P–OH bonds (533.0 eV) to P–O–Ti or P–O–Nb bonds.

Fig. 6 High resolution O1s XPS peak of CAUDPA coated Ti45Nb in the bulk (**a**) and surface sensitive (**b**) modes

Fig. 7 Optical micrographs of osteoblast cell cultures on tested samples after 7 days on (**a**) anodized Ti45Nb and (**b**) RGD-grafted Ti45Nb. Insets: well surface next to the sample
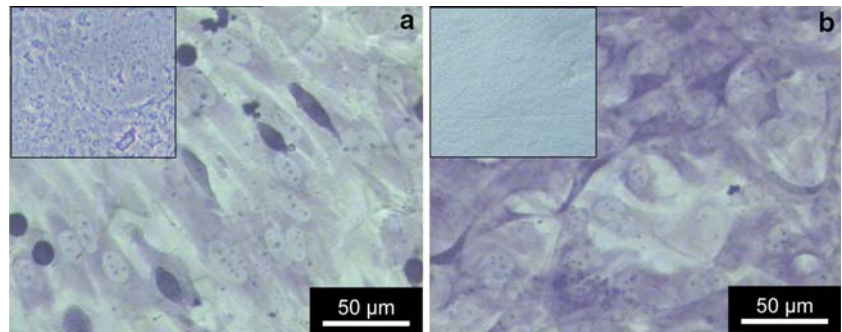

It is also possible to estimate the thickness of the SAM using XPS data from different takeoff angles [26]. The XPS intensity, I, from a smooth substrate covered by a thin film of thickness d is given by the equation: $I = I_0 \exp(-\frac{d}{\lambda \sin \theta})$ where I_0 is the photoelectron intensity from the clean substrate, θ is the emission angle (with respect to the surface) and λ is the attenuation length of the emitted photoelectrons from the substrate. The phosphorous, P $2p_{3/2}$, is at the interface between the monolayer and the substrate so its signal at the two emission angle was used to estimate the thickness of the organic film. The intensities of the P $2p_{3/2}$ used to determine the atomic percentage in Table 1 is 1536 and 556 cps for the bulk and surface sensitive modes, respectively. The attenuation length, λ, calculated as described above, gives a value of 38.8 Å. The dependence between the intensity and the takeoff angle for P $2p_{3/2}$ gives a thickness value, d, of 1.5 nm for the carbon chains above the phosphorous. This compares very favorably with the expected distance of ~1.6 nm between the first and last

carbon of the CAUDPA molecule and speaks strongly for the monolayer character of the organic coat.

These observations correspond well to the model proposed [15] for alkyl phosphates on metal oxide surfaces and support a presence of an alkylphosphonate-anchored SAM on Ti45Nb with phosphonic groups at the SAM-oxide interface in a well-defined orientation, with chloroacetyl functionalities facing the free surface. These chloroacetyl tails of the obtained SAM were further used for binding RGDC peptide to the Ti45Nb surface.

Prior to attaching RGDC, a CAUDPA coated sample was immersed into 70% ethanol to study the possible effects of sterilization on the SAM. FTIR spectrum of the sample after 30 min in ethanol was not different from that of the sample before immersion (Fig. 3) suggesting that the organic monolayer will not be damaged by sterilization. XPS analysis performed following immersion in the RGDC solution and sterilization detected a measurable peak of nitrogen, N1s at 399.6 eV suggesting that a certain amount of

Fig. 8 Scanning electron micrographs of osteoblast cell cultures on tested samples after 7 days on (**a**) anodized Ti45Nb, (**b**) CAUDPA-coated Ti45Nb and (**c**) RGD-grafted Ti45Nb
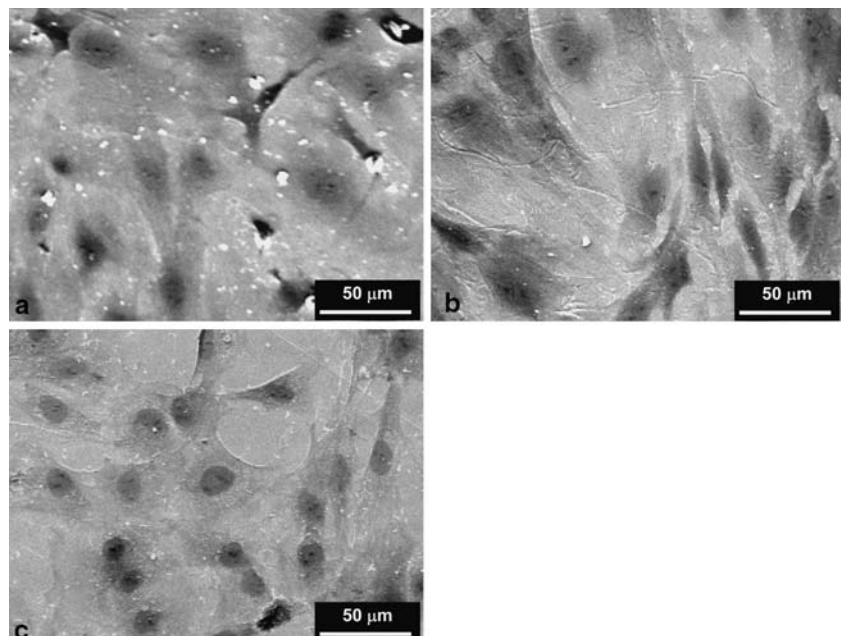
RGDC peptide had attached to the SAM coated Ti45Nb alloy.

Figures 7 and 8 show the surfaces of differently treated Ti45Nb samples after 7 days in osteoblast cell culture. Attached osteoblasts can be seen on all the surface types, however their density on the RGDC-modified alloy, Figs. 7b and 8c, is noticeably higher. It can also be seen in Fig. 8b that CAUDPA coating without the attached RGDC peptide doesn't significantly affect cell density suggesting that cell adhesion is mediated by the peptide itself. Another important observation is that for the bare anodized Ti45Nb, the cells are covering both the alloy sample and the bottom of the polystyrene well, Fig. 7a (inset). In contrast to this, no cells are found on the polystyrene well around the RGDC-grafted alloy, Fig. 7b (inset). In our opinion, this indicates that the cells, seeded selectively on the material surface for the first 10 min, adhered more quickly to the RGD-grafted surface than to the bare alloy, so that very few cells were left when the additional amount of the medium was added, and therefore practically no cells had possibility to access the polystyrene bottom of the well. These qualitative results encourage us to believe that RGDC immobilization can enhance the osteoconductivity of Ti45Nb alloy.

Conclusions

11-chloroacetyl-1-undecylphosphonic acid (CAUDPA) molecules were attached to electropolished and anodically oxidized Ti45Nb alloy surface using a procedure previously developed for the deposition of HDPA self-assembled monolayer (SAM). Wetting, XPS, and FTIR measurements verified the presence of the relatively uniform albeit slightly disordered CAUDPA SAM. The molecules were found to be covalently bound to the substrate in a configuration where the phosphonic groups turn toward the Ti45Nb substrate while the acetyl chloride end group tails face the free surface. Exchanging the chloride with RGDC peptide through the reaction with thiol group present in the peptide terminal cystein allowed the immobilization of RGDC on the metal surface. Cell culture study clearly indicated preferential adhesion of osteoblasts to the RGDC-grafted Ti45Nb surface.

References

1. M. NIINOMI, *Biomaterials* **24** (2003) 2673
2. E. B. TADDEI, V. A. R. HENRIQUES, C. R. M. SILVA and C. A. A. CAIRO, *Mater. Sci. Eng. C* **24** (2004) 683
3. R. GODLEY, D. STAROSVETSKY and I. GOTMAN, *J. Mater. Sci: Mater. Med.* **16** (2005) 1
4. B. KASEMO, *J Prosthet Dent* **49** (1983) 832
5. A. G. GRISTINA, *Science* **237** (1987) 1588
6. E. RUOSLAHTI and M. D. PIERSCHBACHER, *Science* **238** (1987) 491
7. D. M. FERIS, G. D. MOODIE, D. M. DIMOND, C. W. D. GIORANNI, M. G. ERLICH and R. F. VALENTINI, *Biomaterials* **20** (1999) 2323
8. N. BALACHNDER and C. N. SUKENIK, *Langmuir* **6** (1990) 1621
9. C. D. BAIN, E. B. TROUGHTON, Y. T. TAO, J. EVALL, G. M. WHITESIDES, R. G. NUZZO, *J Am Chem Soc* **111** (1989) 321
10. L. H. DUBOIS and R. G. NUZZO, *Ann. Rev. Phys. Chem.* **43** (1992) 437
11. A. ULMAN, *Chem. Rev.* **96** (1996) 1533
12. S. J. XIAO, M. TEXTOR and N. D. SPENCER, *Langmuir* **14** (1998) 5507
13. E. S. GAWALT, M. J. AVALTRONI, M. P. DANAHY, B. M. SILVERMAN, E. L. HANSON, K. S. MIDWOOD, J. E. SCHWARZBAUER and J. SCHWARTZ, *Langmuir* **19** (2003) 200
14. D. BROVELLI, G. HÄHNER, L. RUIZ, R. HOFER, G. KRAUS, A. WALDNER, J. SCHLÖSSER, P. OROSZ-LAN, M. EHART and N. D. SPENCER, *Langmuir* **15** (1999) 4324
15. M. TEXTOR, L. RUIZ, R. HOFER, A. ROSSI, K. FELD-MAN, G. HÄHNER and N. D. SPENCER, *Langmuir* **16** (2000) 3257
16. J. L. FANG, N. J. WU, Z. W. WANG and Y. LI, *Corrosion* **47** (1991) 169
17. J. G. Van ALSTEN, *Langmuir* **15** (1999) 7605
18. E. S. GAWALT, M. J. AVALTRONI, N. KOCH and J. SCHWARTZ, *Langmuir* **17** (2001) 5736
19. J. LAUSMAA, B. KASEMO, H. MATTSSON and H. ODE-LIUS, *App. Surf. Sci.* **45** (1990) 189
20. J. LAUSMAA, B. KASEMO, U. ROLANDER, L. M. BJURSTEN, L. E. ERICSON, L ROSANDER, P. THOM-SEN, in ''Surface Characterization of Biomaterials'', edited by B. D. Ratner (Elsevier, 1988) p. 161
21. Y. SAHOO, H. PIZEM, T. FRIED, D. GOLODNITSKY, L. BURSTEIN, C. N. SUKENIK and G. MARKOVICH, *Langmuir* **17** (2001) 7907
22. G. ZORN, I. GOTMAN, E. Y. GUTMANAS, R. ADADI, G. SALITRA and C. N. SUKENIK, *Chem. Mater.* **17** (2005) 4218
23. S. TOSATTI, R. MICHEL, M. TEXTOR and N. D. SPENCER, *Langmuir* **18** (2002) 3537
24. Y. WADA, H. KATAOKA, S. YOKOSE, T. ISHIZUYA, K. MIYAZONO, Y. -H. GAO, Y. SHIBASAKI and A. YAMAGUCHI, *Bone* **22** (1998) 479
25. G. ZORN, A. LESMAN, I. GOTMAN, *Surface Coat. Techn.*, (in press)
26. H. YAMAMOTO, R. A. BUTERA, Y. GU and D. H. WALDECK, *Langmuir* **15** (1999) 8640